Am J Physiol Renal Physiol 313: F561–F575, 2017.
First published February 22, 2017; doi:10.1152/ajprenal.00036.2017.

RESEARCH ARTICLE | *Mechanism and Treatment of Renal Fibrosis*

Inhibiting aerobic glycolysis suppresses renal interstitial fibroblast activation and renal fibrosis

Hao Ding,[1]* Lei Jiang,[1]* Jing Xu,[1] Feng Bai,[1] Yang Zhou,[1] Qi Yuan,[1] Jing Luo,[1] Ke Zen,[2] and Junwei Yang[1]*

[1]*Center for Kidney Disease, Second Affiliated Hospital, Nanjing Medical University, Nanjing, China; and* [2]*State Key Laboratory of Pharmaceutical Biotechnology, Nanjing University Advanced Institute of Life Sciences, Nanjing, China*

Submitted 24 January 2017; accepted in final form 15 February 2017

Ding H, Jiang L, Xu J, Bai F, Zhou Y, Yuan Q, Luo J, Zen K, Yang J. Inhibiting aerobic glycolysis suppresses renal interstitial fibroblast activation and renal fibrosis. *Am J Physiol Renal Physiol* 313: F561–F575, 2017. First published February 22, 2017; doi: 10.1152/ajprenal.00036.2017.—Chronic kidney diseases generally lead to renal fibrosis. Despite great progress having been made in identifying molecular mediators of fibrosis, the mechanism that governs renal fibrosis remains unclear, and so far no effective therapeutic antifibrosis strategy is available. Here we demonstrated that a switch of metabolism from oxidative phosphorylation to aerobic glycolysis (Warburg effect) in renal fibroblasts was the primary feature of fibroblast activation during renal fibrosis and that suppressing renal fibroblast aerobic glycolysis could significantly reduce renal fibrosis. Both gene and protein assay showed that the expression of glycolysis enzymes was upregulated in mouse kidneys with unilateral ureter obstruction (UUO) surgery or in transforming growth factor-β1 (TGF-β1)-treated renal interstitial fibroblasts. Aerobic glycolysis flux, indicated by glucose uptake and lactate production, was increased in mouse kidney with UUO nephropathy or TGF-β1-treated renal interstitial fibroblasts and positively correlated with fibrosis process. In line with this, we found that increasing aerobic glycolysis can remarkably induce myofibroblast activation while aerobic glycolysis inhibitors shikonin and 2-deoxyglucose attenuate UUO-induced mouse renal fibrosis and TGF-β1-stimulated myofibroblast activation. Furthermore, mechanistic study indicated that shikonin inhibits renal aerobic glycolysis via reducing phosphorylation of pyruvate kinase type M2, a rate-limiting glycolytic enzyme associated with cell reliance on aerobic glycolysis. In conclusion, our findings demonstrate the critical role of aerobic glycolysis in renal fibrosis and support treatment with aerobic glycolysis inhibitors as a potential antifibrotic strategy.

chronic kidney disease; fibroblast; fibrosis; aerobic glycolysis

CHRONIC KIDNEY DISEASE (CKD) has become a major public health threat on a global scale and imposed enormous socioeconomic burdens. An estimated 13–16% of the adult population worldwide has various degrees of CKD and may need renal replacement therapy with dialysis and/or kidney transplant at some point in the future (17, 54). Regardless of the underlying disorder and whether the injury is sustained, the kidney will follow a doomsday path of renal fibrosis, a condition characterized by a loss of capillary networks (48) and an accumulation of fibrillar collagens (2, 10, 39), interstitial inflammatory response (8, 13, 16, 31), and activated interstitial fibroblasts (15a). This excessive matrix deposition eventually leads to tissue destruction and impairment of renal function. Despite extensive efforts to identify the critical cellular and molecular mediators of renal fibrosis, the final common pathway of a wide variety of CKD (26), the mechanisms that govern renal fibrosis remain incompletely understood, and currently there is no effective clinical treatment to stop the progression of renal fibrosis.

Fibroblast proliferation and extracellular matrix synthesis are major contributors to the progression of interstitial fibrosis. A variety of studies have identified myofibroblasts as the primary source of the scar-forming matrix proteins, such as collagens, fibronectins (FN), elastins, and fibrillins, which contribute to fibrosis (12, 24, 32, 41, 47). Fibroblast activation, a transformation process from quiescent interstitial cells to proliferating and excessively matrix-producing cells, typically occurs through stimulation by growth factors, direct cell-cell contacts, extracellular matrix via integrins, and environmental conditions such as hyperglycemia or hypoxia in renal disease. Direct targeting of fibroblast activation by various inhibitors has proved successful in experimental models and thus may lead to new approaches in the treatment of progressive renal disease (22, 25, 40, 56). Recently, energy metabolism became a particularly interesting topic in kidney disease research because the kidney is one of the organs with the highest metabolic rate in the body (46). Both clinical studies and experimental studies have indicated that metabolic perturbation is involved in various CKD (9, 35, 38, 53), including diabetic kidney disease (30, 34) and polycystic kidney disease (5, 37). For example, Yu et al. (53) applied a commercial liquid chromatography-mass spectrometry/gas chromatography-mass spectrometry (LC-MS/GC-MS)-based platform to measure 204 metabolites in plasma from 1,921 African American participants and found that lower levels of 5-oxoproline and 1,5-anhydroglucitol were associated with new-onset CKD. Employing the same LC-MS/GC-MS-based platform, Posada-Ayala et al. (35) demonstrated that a panel of 7 urinary metabolites could serve as a marker to separate CKD patients from 30 individuals without CKD. In addition, Niewczas et al. (30) performed the first study to examine the relation between plasma metabolite levels and progression to end-stage renal disease (ESRD), in which they measured 262 plasma metabolites in 80 individuals over 8–12 yr of follow-up and found that *p*-cresol sulfate, several polyols, and nucleotide derivatives

* H. Ding and L. Jiang contributed equally to this work.

Address for reprint requests and other correspondence: J. Yang, Center for Kidney Disease, Second Affiliated Hospital, Nanjing Medical Univ., 262 N. Zhongshan Rd., Nanjing, Jiangsu 210003, China (e-mail: jwyang@njmu.edu.cn).

were associated with an increased risk of progression to ESRD. In a study of early diabetic nephropathy, Pena et al. (34) indicated that several plasma (histidine and butenoylcarnitine) and urine (hexose, glutamine, and tyrosine) metabolites were associated with the transition from microalbuminuria to macroalbuminuria. Rowe et al. (37) observed that *Pkd1*$^{-/-}$ cells acidify culture media more rapidly than wild-type cells and that *PKD1* deletion causes a switch to aerobic glucose metabolism. Intriguingly, the authors showed that inhibiting glycolysis with 2-deoxyglucose (2-DG) reduced cyst growth in two distinct mouse models of polycystic kidney disease (PKD), revealing a shift toward aerobic glycolysis in PKD pathogenesis. However, there is little information available regarding the role of kidney cell metabolism profile change in renal fibrosis. The questions as to whether aerobic glycolysis is required for renal myofibroblast activation and whether modulation of renal fibroblast aerobic glycolysis can affect the occurrence and progression of renal fibrosis still remain to be addressed.

In the present study, we demonstrated for the first time that altered glucose metabolism is the primary feature of renal myofibroblast activation during kidney fibrosis. The key enzymes that catalyze glycolytic reactions are upregulated in transforming growth factor-β1 (TGF-β1)-treated normal rat kidney interstitial fibroblast (NRK-49F) cells and fibrotic kidney tissues. Furthermore, this study suggests that inhibition of aerobic glycolysis is an effective approach to suppress renal fibrosis and thus provides a potential novel therapeutic strategy in treating CKD.

MATERIALS AND METHODS

Mice and animal models. Male CD-1 mice weighing ~18–22 g were acquired from the Specific Pathogen-Free Laboratory Animal Center of Nanjing Medical University and maintained according to the guidelines of the Institutional Animal Care and Use Committee at Nanjing Medical University. 2-DG was administered intraperitoneally at a dose of 100 mg/kg body wt 1 day before unilateral ureter obstruction (UUO) surgery, and 2-DG was administered for 7 consecutive days. Unilateral kidneys were injected with lentiviral pyruvate kinase muscle (PKM) RNAi or lentiviral control designed by Genechem (Shanghai, China) 3 days before UUO surgery. The retroperitoneum was opened, and the left kidney was exposed. Then, 5×10^7 transducing units (TU) PKM RNAi lentiviral vectors were injected into the lower pole of the left kidney at several sites. Shikonin (catalog no. S7576; Sigma-Aldrich) was intragastrically administered at a dose of 1 or 5 mg/kg body wt 1 day before UUO surgery, and shikonin was administered for 7 consecutive days. UUO was performed using an established protocol, as described previously. Sham-operated mice were used as normal controls. The UUO kidneys were harvested at 7 days after surgery. One portion of the kidney was fixed in 10% phosphate-buffered formalin, followed by paraffin embedding for histological and immunohistochemical staining. Another portion was immediately frozen in Tissue-Tek optimum cutting temperature compound (Sakura Finetek, Torrance, CA) for cryosection. The remaining kidney tissue was snap-frozen in liquid nitrogen and stored at −80°C for extraction of RNA and protein.

Human subjects. Human renal biopsy samples were collected from individuals with different degrees of renal fibrosis at the Center for Kidney Disease of Second Affiliated Hospital of Nanjing Medical University. For analysis of human subjects, written informed consent was obtained from everyone, and the study protocol conformed to the ethical guidelines of the 1975 Declaration of Helsinki as reflected in a priori approval by the Ethics Committees of Nanjing Medical University for Medical Experiments.

Cell culture and treatment. Normal rat kidney interstitial fibroblast cells (NRK-49F) were obtained from American Type Culture Collection (Manassas, VA). Cells were cultured in Dulbecco's modified Eagle's medium/F12 medium supplemented with 10% fetal bovine serum (Invitrogen, Grand Island, NY). The NRK-49F cells were seeded on six-well culture plates to 60–70% confluence in the complete medium containing 10% fetal bovine serum for 16 h and then changed to serum-free medium after washing twice with medium. After serum starvation for 16 h, cells were exposed to the treatment for the indicated time periods before harvesting and subjecting them to Western blotting, reverse transcriptase PCR (RT-PCR), or immunofluorescence staining, respectively. Human recombinant transforming growth factor-β1 (TGF-β1; 2 ng/ml; catalog no. 100-B-010-CF; R&D, Minneapolis, MN), human recombinant pyruvate kinase type M2 (PKM2; catalog no. SAE0021; Sigma-Aldrich), and lactic acid (catalog no. L1750; Sigma-Aldrich) were added to the serum-free medium for indicated time periods and at indicated concentration. 2-DG (catalog no. D8375; Sigma-Aldrich) and dichloroacetic acid (catalog no. 36545; Sigma-Aldrich) were added to the serum-free medium for indicated time periods and at indicated concentration 30 min before TGF-β1 treatment. NRK-49F cells were transfected with lentiviral PKM2 RNAi designed by Genechem according to the manufacturer's instructions. PKM2 plasmid designed by Genechem was transfected into NRK-49F cells using Lipofectamine 2000 reagent (Invitrogen) according to the manufacturer's instructions.

Western blot analysis. Cultural NRK-49F cells were lysed in 1× SDS sample buffer. The kidneys were lysed with radioimmunoprecipitation assay solution containing 1% NP-40, 0.1% SDS, 100 mg/ml PMSF, 1% protease inhibitor cocktail, and 1% phosphatase I and II inhibitor cocktail (Sigma, St. Louis, MO) on ice. The supernatants were collected after centrifugation at 13,000 *g* at 4°C for 30 min. Protein concentration was determined by bicinchoninic acid protein assay (BCA Kit; Pierce Thermo-Scientific, Rockford, IL) according to the manufacturer's instructions. An equal amount of protein was loaded into 10 or 12% SDS-PAGE and transferred onto polyvinylidene difluoride membranes. The primary antibodies were as follows: anti-phospho-PKM2 (Tyr105; catalog no. 3827S; Cell Signaling Technology), anti-PKM2 (catalog no. ab38237; Abcam), anti-PCNA (catalog no. sc-56; Santa Cruz Biotechnology), anti-FN (catalog no. F3648; Sigma-Aldrich), anti-collagen-α1 type 1 (COL1A1; catalog no. sc-25974; Santa Cruz Biotechnology), anti-α-smooth muscle actin (α-SMA; catalog no. ab124964; Abcam), and anti-α-tubulin (catalog no. T6074; Sigma-Aldrich).

RNA isolation and real-time quantitative reverse transcriptase PCR. Total RNA was extracted using TRIzol reagent (Invitrogen) according to the manufacturer's instructions. cDNA was synthesized with 1 μg of total RNA, ReverTra Ace (Vazyme, Nanjing, China), and oligo(dT)$_{12–18}$ primers. Gene expression was measured by real-time PCR assay (Vazyme) and 7300 Real-Time PCR System (Applied Biosystems, Foster City, CA). The relative amount of mRNA or gene to internal control was calculated using the expression 2ΔCT, in which $\Delta CT = CT_{gene} - CT_{control}$, and CT is cycle threshold.

Lactate, glucose assay, and pH measurement. Lactate concentration of cell supernatant was measured using Lactate Colorimetric/Fluorometric Assay Kit (K607-100; Biovision). Glucose concentration of cell supernatant was measured using Glucose Colorimetric/Fluorometric Assay Kit (K606-100; Biovision). The pH of cell supernatant was measured with a pH instrument (LE438; Mettler Toledo) according to the manufacturer's instructions.

Seahorse XF24 mitochondrial stress analysis and glycolysis analysis. Optimization of cell density and working concentration titers for each individual inhibitor was completed before the Seahorse XF24 mitochondrial stress analysis according to the Seahorse XF24 User's Manual (Seahorse Bioscience, Billerica, MA). Oxygen consumption rate and extracellular acidification rate were automatically calculated, recorded, and plotted by Seahorse XF24 software version 1.8 (Seahorse Bioscience). At the end of each assay, cells were washed once

with an excess of room temperature Dulbecco's PBS and lysed with ice-cold radioimmunoprecipitation assay buffer (0.15 M NaCl, 1 mM EDTA, 1 mM EGTA, 0.5% sodium deoxycholate, 0.1% SDS, 1% Triton X-100, 50 mM Tris-HCl, pH 7.8, and protease and phosphatase inhibitor cocktails), and the protein content was estimated by Bio-Rad DC Protein Assay (Bio-Rad, Hercules, CA) using a Molecular Devices Softmax M3 microplate reader (Sunnyvale, CA). Data were normalized for total protein content per well. Additional details relating to the Seahorse XF24 analyzer can also be found at http://www.agilent.com/en-us/promotions/xftechnologyoverview.

Quantitative determination of collagen in kidney tissue. Three-micrometer-thick sections of paraffin-embedded tissue were stained with Sirius red F3BA and Food green FCF (Sigma-Aldrich) overnight. After washing three times with 1× PBS buffer, the dye was eluted from tissue sections with 0.1 N sodium hydroxide methanol. Absorbance at 540 and 605 nm was determined for Sirius red F3BA and Food green FCF-binding protein, respectively. This assay provides a simple, relative measurement of the ratio of collagen to total protein, which is expressed as micrograms per milligram of total protein.

Histology and immunohistochemistry. Kidney samples were fixed in 10% neutral formalin and embedded in paraffin. Three-micrometer-thick sections were used for hematoxylin and eosin, periodic acid-Schiff, and Masson staining. For immunohistochemical staining, paraffin-embedded kidney sections were deparaffinized, hydrated, and antigen retrieved, and endogenous peroxidase activity was quenched by 3% H_2O_2. Sections were then blocked with 10% normal donkey serum, followed by incubation with anti-PKM2 (catalog no. ab38237; Abcam), anti-α-SMA (catalog no. ab124964; Abcam), or anti-PCNA (catalog no. sc-56; Santa Cruz Biotechnology) overnight at 4°C. After incubation with secondary antibody for 1 h, sections were incubated with avidin-biotin complex reagents for 1 h at room temperature before being subjected to substrate 3-amino-9-ethylcarbazole or 3,3′-diaminobenzidine (Vector Laboratories, Burlingame, CA). Slides were viewed with a Nikon Eclipse 80i microscope equipped with a digital camera (DS-Ri1; Nikon, Shanghai, China).

Immunofluorescent staining. Kidney cryosections at 3-μm thickness were fixed for 15 min in 4% paraformaldehyde, followed by permeabilization with 0.2% Triton X-100 in PBS for 5 min at room temperature. After blocking with 2% donkey serum for 60 min, the slides were immunostained with anti-PKM2 (catalog no. ab38237; Abcam), anti-FN (catalog no. F3648; Sigma-Aldrich), or anti-α-SMA (catalog no. ab124964; Abcam). 4′,6-diamidino-2-phenylindole (DAPI) was used to visualize the nuclei. Cells cultured on coverslips were washed twice with cold 1× PBS and fixed with cold methanol/acetone (1:1) for 10 min at −20°C. After three extensive washings with 1× PBS, the cells were treated with 0.1% Triton X-100 for 5 min, blocked

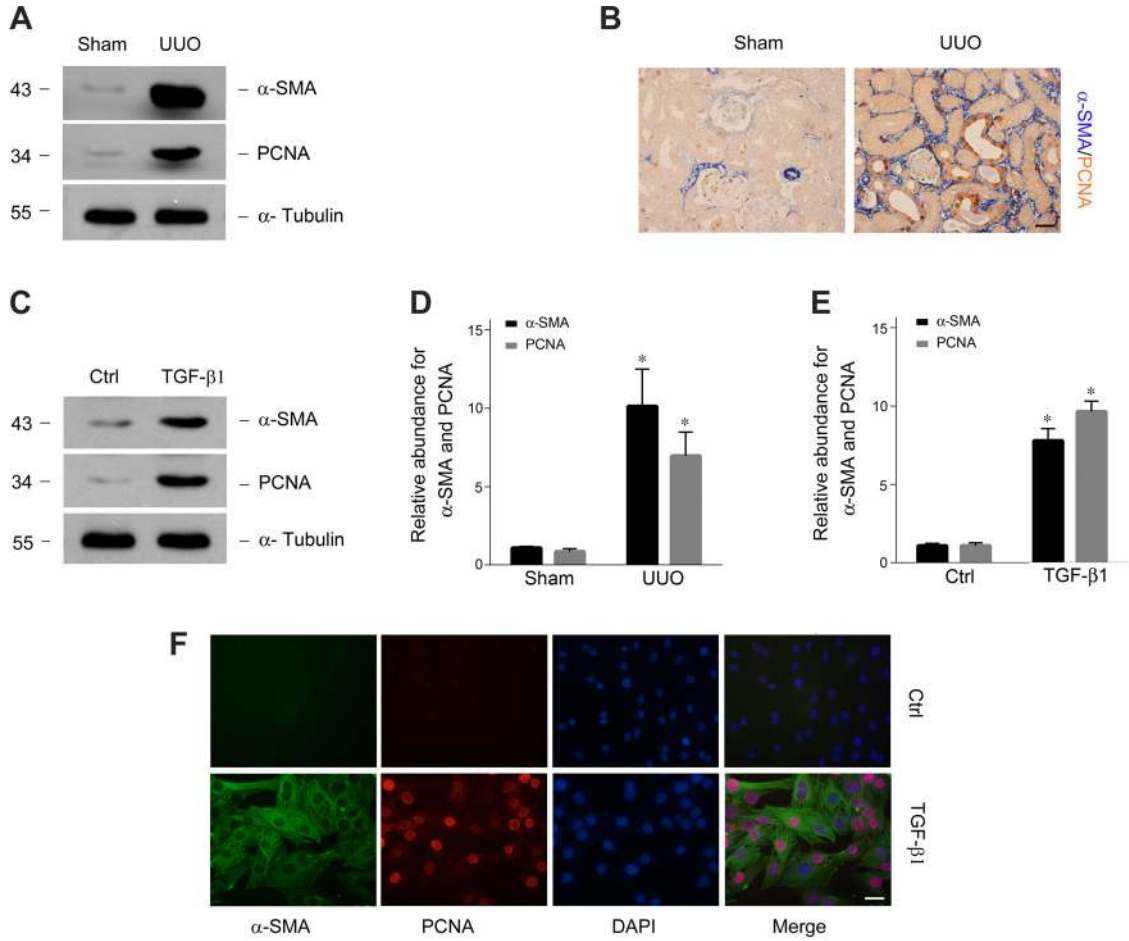

Fig. 1. TGF-β1 induces fibroblast proliferation and activation. *A*: Western blot analysis of α-SMA and PCNA in the kidneys with UUO nephropathy or sham control. Kidneys were collected on *day 7* after UUO. *B*: representative immunohistochemical staining for α-SMA and PCNA in the kidneys of sham control and fibrotic kidney induced by UUO nephropathy. Blue indicates α-SMA staining, and brown indicates PCNA staining. Scale bar = 20 μm. *C*: Western blot analysis of α-SMA and PCNA level in NRK-49F cells incubated with or without TGF-β1 (2 ng/ml) for 48 h. *D*: graphic presentation of kidney α-SMA and PCNA levels normalized to α-tubulin. $^*P < 0.05$ compared with sham controls ($n = 3$). *E*: graphic presentation of α-SMA and PCNA levels in NRK-49F cells normalized to α-tubulin. $^*P < 0.05$ compared with controls ($n = 3$). *F*: representative immunostaining for α-SMA and PCNA in NRK-49F cells treated with or without TGF-β1 (2 ng/ml) for 48 h. Cells were costained with DAPI to visualize the nuclei. Scale bar = 10 μm. Ctrl, control.

with 2% normal donkey serum in 1× PBS buffer for 40 min at room temperature, and incubated with the anti-α-SMA or anti-PKM2 followed by staining with fluorescein isothiocyanate or tetramethylrhodamine-conjugated secondary antibody. Cells were also stained with DAPI to visualize the nuclei. Slides were viewed with a Nikon Eclipse 80i Epi-fluorescence microscope equipped with a digital camera (DS-Ri1; Nikon, New York, NY).

Statistical analysis. Western blotting, RT-PCR, and immunofluorescence staining were all repeated at least three times independently. For the histologic analysis and immunostaining, quantification was performed using Image-Pro Plus 6.0 software. For Western blot analysis, quantitation was performed by scanning and analyzing the intensity of the hybridization signals using National Institutes of Health Image software. All data examined are presented as means ± SE. Statistical analysis of the data was performed using SigmaStat software (Jandel Scientific Software, San Rafael, CA). Comparisons between groups were made using one-way ANOVA, followed by Student's *t*-test. $P < 0.05$ was considered statistically significant.

RESULTS

Increase of aerobic glycolysis and phosphorylated PKM2 level inactivated myofibroblasts during renal fibrosis. In the present study, we employed mice with unilateral ureter obstruction (UUO) and TGF-β1-treated kidney interstitial fibroblast cells as two model systems to characterize whether altered glucose metabolism is a feature of the activated myofibroblasts in renal fibrosis. As the renal interstitial fibroblast activation and proliferation is central to the development of renal fibrosis after different insults, we first examined the renal interstitial fibroblast activation in the UUO-induced fibrotic kidneys. As shown in Fig. 1, *A* and *D*, Western blot analysis confirmed that the expression of α-smooth muscle actin (α-SMA) and PCNA in the fibrotic kidneys was significantly higher compared with sham control. Double immunohistochemical staining with antibodies against α-SMA and PCNA indicated that significantly more α-SMA-positive fibroblasts in the renal interstitium are proliferating (PCNA-positive; Fig. 1*B*), confirming that myofibroblast activation was accompanied by increase of proliferation. Proliferation and activation of renal fibroblasts promoted by TGF-β1 were also monitored. In this experiment, NRK-49F cells, a rat kidney interstitial fibroblast cell line, were treated with TGF-β1 (2 ng/ml) for 48 h. As shown in Fig. 1, *C* and *E*, TGF-β1 remarkably induced the cell proliferation marked by PCNA, and the proliferated fibroblasts expressed high level of α-SMA. Double immunofluorescence staining with antibodies against α-SMA and PCNA in TGF-β1-treated NRK-49F cells also confirmed the results of Western blot assay (Fig. 1*F*).

The metabolic derangement observed in a number of chronic kidney diseases prompted us to examine whether aerobic glycolysis is a feature of the activated myofibroblasts in renal fibrosis. We first examined the gene related to glycolysis by quantitative RT-PCR and found that these genes were upregulated in the fibrotic kidney compared with kidney tissue obtained from sham controls (Fig. 2*A*). It is generally believed that PKM2 serves as the final rate-limiting enzyme associated with cell reliance on aerobic glycolysis (51). Through phosphorylation particularly at Tyr105, PKM2 can form a dimer, which is catalytically inactive for conversion of phosphoenolpyruvic acid to pyruvate and production of ATP, and thus force the cell to switch metabolism to aerobic glycolysis (44). Given the critical role of PKM2 in controlling cell glycolysis, we next detected the level of PKM2, particularly phosphorylated PKM2, at Tyr105 (p-PKM2) in the fibrotic kidneys 1, 3, and 7 days after the UUO procedure. Western blot analysis indicated that the levels of both PKM2 and p-PKM2 in fibrotic kidneys were markedly increased compared with kidney tissues from sham control (Fig. 2*B*). The elevation of PKM2 levels in fibrotic kidneys was further confirmed by immunohistochemical staining. As shown in Fig. 2*C*, PKM2 was induced during renal fibrosis, and the inducted PKM2 was largely localized in the interstitium of the fibrotic kidneys.

To test whether this upregulation of aerobic glycolysis as well as PKM2 levels in kidney tissues also occurs in patients with nephropathy, we examined renal biopsy samples from individuals with different degrees of renal fibrosis. The biopsy samples were collected from Center for Kidney Disease, Second Affiliated Hospital, Nanjing Medical University, from 2010 to 2016. The amount of fibrosis in these sections was analyzed by trichrome staining. It was graded as 0, 1, 2, or 3 if the percentage of fibrosis in the kidney tissue section was <5,

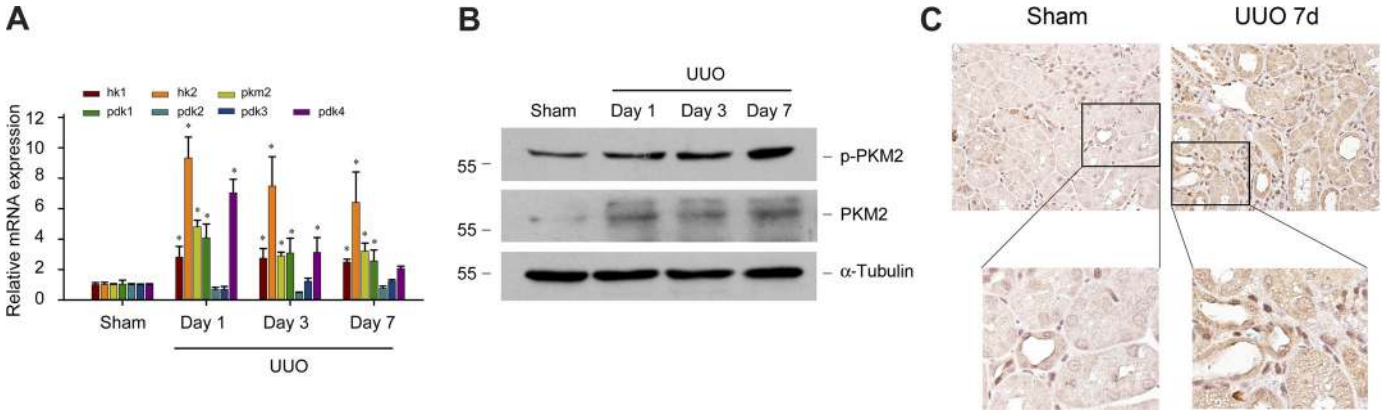

Fig. 2. Glycolysis-related genes and proteins were upregulated in fibrotic kidneys. *A*: quantitative real-time RT-PCR analysis displayed the relative levels of mRNA transcripts involved in glycolysis in the kidneys with UUO nephropathy compared with sham control.*$P < 0.05$ compared with sham controls ($n = 3$). *B*: Western blot analysis showing the expression of p-PKM2 and PKM2 in the fibrotic kidneys compared with sham control. Kidney tissue lysates were immunoblotted with antibodies against p-PKM2 and PKM2, or α-tubulin, respectively. *C*, *top*: representative immunohistochemical staining for PKM2 in the kidney interstitium of sham control and fibrotic kidney. *Bottom*: higher magnifications of boxed areas in images at *top*. Here, d, days.

6–25, 26–50, or >50%, respectively. As shown by immunohistochemical analysis in Fig. 3*A*, a significant amount of PKM2-positive myofibroblasts were accumulated within the renal interstitium. Furthermore, the number of PKM2-positive myofibroblasts in those individuals with severe renal fibrosis was higher than those with less renal fibrosis (Fig. 3*B*). We also examined relative normal kidney tissues from patients with renal carcinoma and found that there was almost no PKM2-positive myofibroblast in renal interstitium (data not shown). Taken together, these results suggest that the progression of renal fibrosis is tightly correlated with the increase of aerobic glycolysis in kidney tissues.

We next examined the correlation between fibrosis and aerobic glycolysis by using NRK-49F fibroblast treated with or without 2 ng/ml TGF-β1. Similarly, the expression levels of genes involved in glycolysis were significantly higher in the TGF-β1-treated NRK-49F cells compared with control cells (Fig. 4*A*). Furthermore, the increase of aerobic glycolysis in TGF-β1-treated myofibroblasts was supported by results from the immunofluorescent staining experiments. As shown in Fig. 4*B*, the expression of PKM2 and α-SMA in NRK-49F cells was remarkably increased after 48-h treatment with TGF-β1. Western blot analysis further showed the rapid increase of phosphorylated PKM2 (p-PKM2) level in TGF-β1-treated

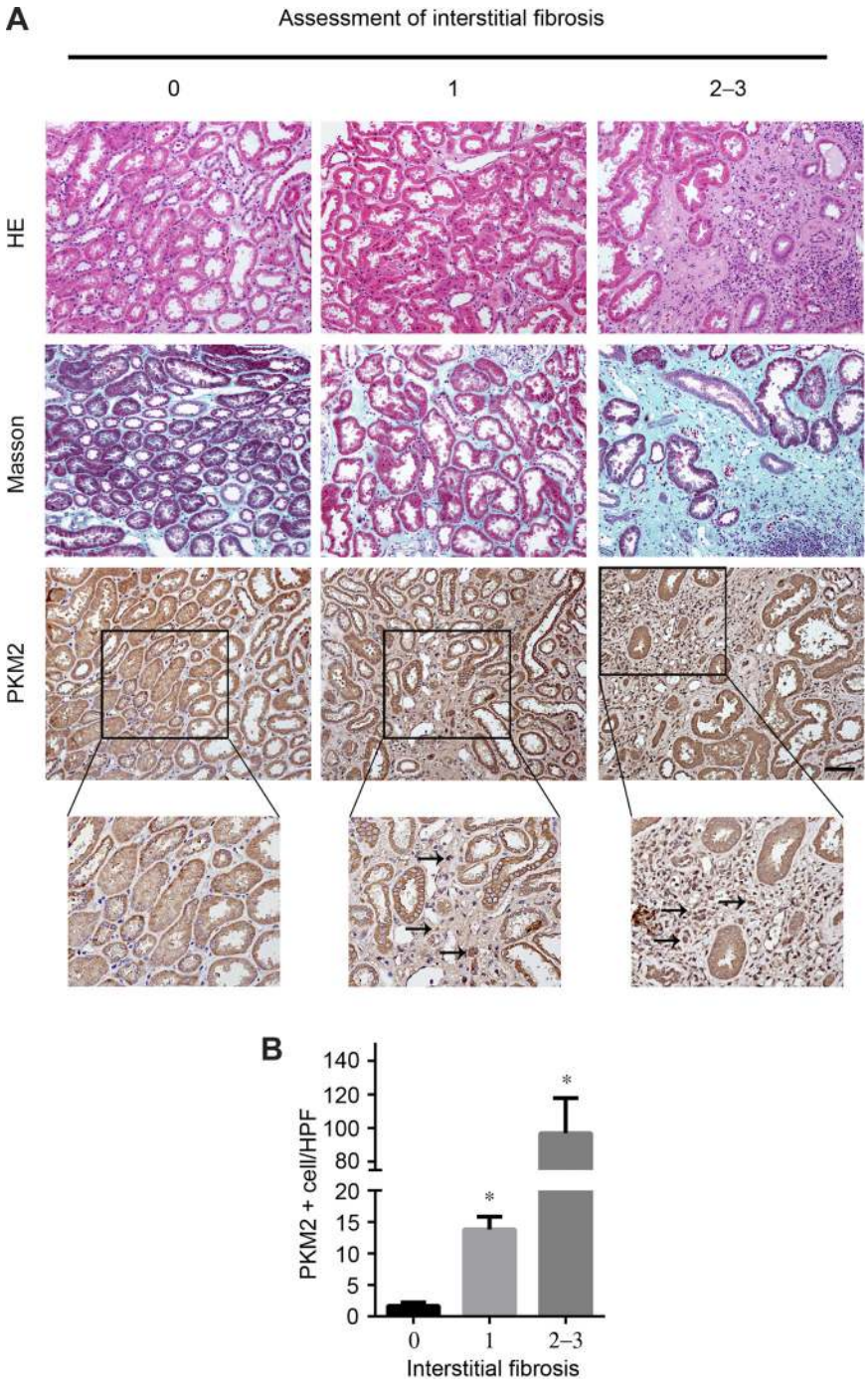

Fig. 3. Renal interstitial fibrosis in patients was correlated with PKM2 expression in kidneys. *A*: representative hematoxylin and eosin (HE) and Masson staining for kidney morphology and interstitial fibrosis and immunohistochemical staining for PKM2 expression in renal interstitial samples from patients with different degrees of renal fibrosis. Higher magnifications of kidney interstitial samples (boxed areas in images at *top*) are shown in the panel at *bottom*. Arrows indicate PKM2-positive interstitial cells. The amount of interstitial fibrosis in these sections was graded on the basis of Masson staining as 0 (if ≤5%), 1 (if 6–25%), 2 (if 26–50%), or 3 (if >50%). *B*: percentage of PKM2-positive interstitial cells in the kidneys from patients with different degrees of renal fibrosis. $*P < 0.05$ compared with *grade 0* controls ($n = 6–8$). Scale bar = 50 μm. HPF, high-power field.

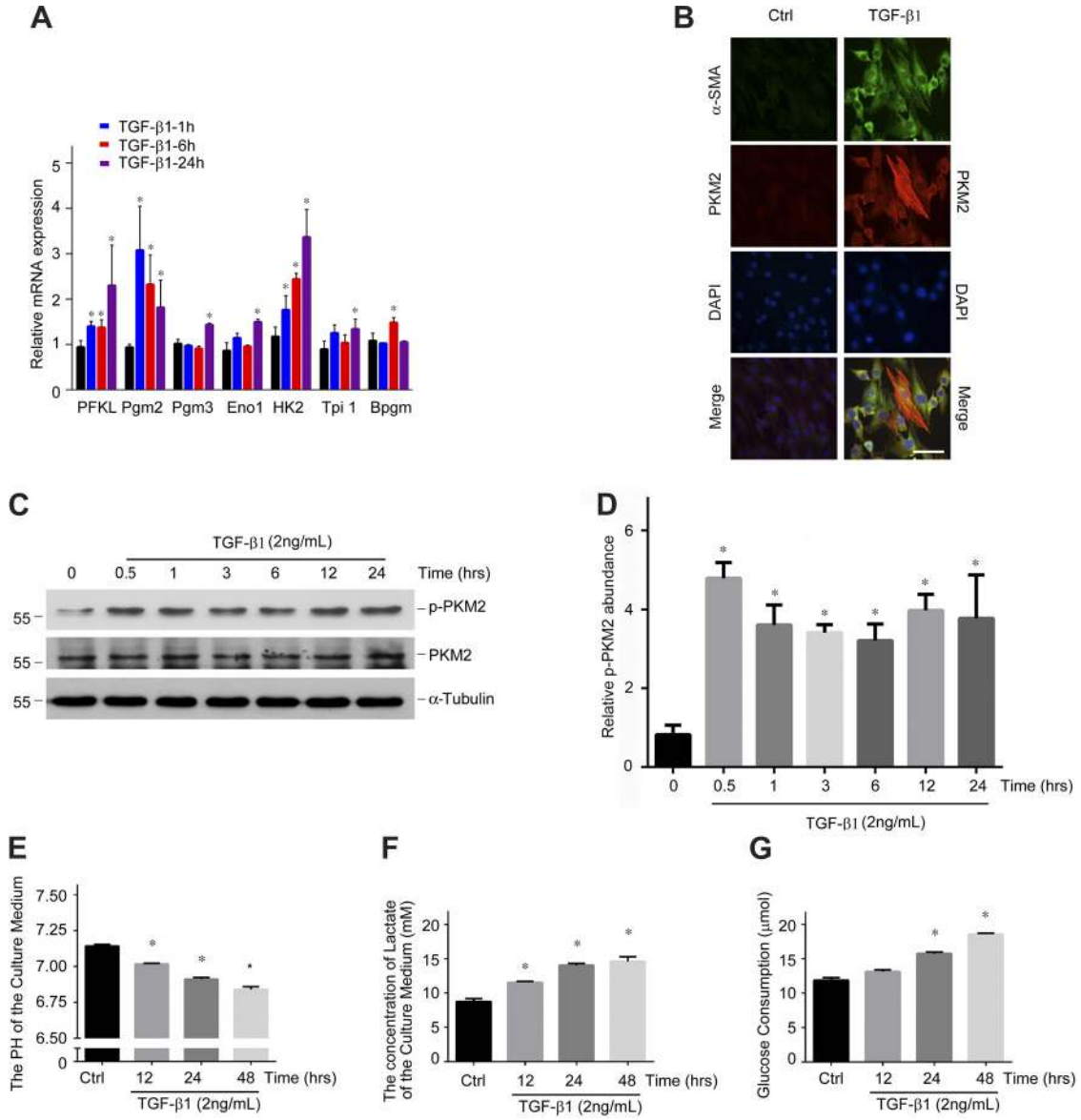

Fig. 4. Glycolysis-related genes and proteins were upregulated in TGF-β1-treated renal myofibroblasts. *A*: quantitative real-time RT-PCR analysis displayed the relative levels of mRNA involved in glycolysis in the NRK-49F cells incubated with or without TGF-β1 (2 ng/ml) for 1, 6, or 24 h. $^*P < 0.05$ compared with controls ($n = 3$). *B*: representative immunofluorescence staining images for α-SMA and PKM2 in NRK-49F cells treated with TGF-β1 (2 ng/ml) for 48 h. Cells were costained with DAPI to visualize the nuclei. Scale bar = 10 μm. *C*: Western blot analysis of p-PKM2 and PKM2 in the TGF-β1-treated NRK-49F cells compared with control cells. Cell lysates were immunoblotted with antibodies against p-PKM2, PKM2, or α-tubulin. *D*: graphic presentation showing the changes for p-PKM2 (Tyr105) normalized to PKM2. *E–G*: NRK-49F cells were treated with or without TGF-β1 for 12, 24, or 48 h. The pH (*E*) and lactate content (*F*) in culture medium and glucose consumption in NRK-49F cells (*G*) were determined. $^*P < 0.05$ compared with controls ($n = 6–8$).

myofibroblasts (Fig. 4, *C* and *D*). The elevation of p-PKM2 in TGF-β1-treated myofibroblasts supports the observation of increase in aerobic glycolysis in these cell types because phosphorylation of PKM2 particularly at Tyr105 will result in formation of catalytically inactive PKM2 dimer and force the cell to switch metabolism to aerobic glycolysis (44). Glucose metabolism assessment confirmed the increase of aerobic glycolysis in myofibroblasts by TGF-β1 treatment. As shown, the pH in the NRK-49F fibroblast culture medium (Fig. 4*E*) was decreased by TGF-β1 treatment in a dose-dependent manner. Direct measurement of extracellular lactate content (Fig. 4*F*) and glucose consumption (Fig. 4*G*) of NRK-49F cells demonstrated that TGF-β1 treatment dose-dependently increased both lactate production and glucose consumption in NRK-49F cells. Taken together, these results suggest that TGF-β1-induced activation and fibrosis in renal myofibroblasts are also associated with increased cellular aerobic glycolysis.

The above data revealed that enhanced glycolysis may participate in the activation of renal myofibroblasts; we wonder whether increased aerobic glycolysis is sufficient to cause myofibroblast activation. Li et al. (23) demonstrated that PKM2 increased endothelial cell proliferation, migration, and cell-extracellular matrix adhesion and promoted tumor angiogenesis by using recombinant human PKM2 (referred to as rPKM2). Gao et al. found that phosphorylation of Stat3 by rPKM2 was dramatically increased (14). First, we employed

the bacterially expressed rPKM2 to treat NRK-49F cells and found that rPKM2 treatment dose-dependently induced FN expression (Fig. 5*A*). rPKM2 also induced FN, α-SMA, and PCNA expression in a time-dependent manner, revealing that rPKM2 can cause myofibroblast activation (Fig. 5*B*). To further investigate whether PKM2 can sufficiently induce myofibroblast activation, a PKM2 mammalian expression plasmid was constructed and transfected into NRK-49F cells. As shown in Fig. 5*C*, PKM2 expression was significantly increased in a dose-dependent manner, and myofibroblasts with PKM2 overexpression, similar to TGF-β1 stimulation and FN expression, were dose-dependently induced (Fig. 5*C*). Transfection of 20-μg PKM2 plasmid could induce FN, α-SMA, and PCNA expression for 72 h (Fig. 5*D*), and extracellular lactate content normalized to protein was significantly increased with PKM2 overexpression (Fig. 5*E*). Furthermore, Western blotting results showed that lactic treatment dose-dependently induced FN expression, and FN, α-SMA, and PCNA expression were markedly upregulated at 24 h and reached a peak at 48 h after lactate treatment (Fig. 5, *F* and *G*). Taken together, these findings indicated that increasing aerobic glycolysis can remarkably induce myofibroblast activation.

Inhibition of aerobic glycolysis attenuates TGF-β1-stimulated myofibroblast activation and UUO-induced renal fibrosis. To confirm the switch of glucose metabolism from oxidative phosphorylation to aerobic glycolysis in TGF-β1-treated NRK-49F fibroblasts, we examined the metabolic status of NRK-49F cells treated with or without TGF-β1 using Seahorse X24 Extracellular Flux Analyzer (11). As shown, extracellular acidification rate (ECAR) (Fig. 6*A*) and glycolytic capacity (Fig. 6*B*) in NRK-49F cells were markedly increased after 24-h treatment with TGF-β1. In contrast, oxygen consumption rate (OCR; Fig. 7*A*), a representation of mitochondrial respiratory activity, maximal respiration (Fig. 7*B*), and ATP production (Fig. 7*C*) were significantly decreased in NRK-49F cells with TGF-β1 treatment for 24 h. Moreover, we found that the ratio of ECAR to OCR was increased in TGF-β1-treated NRK-49F cells compared with controls (Fig. 6*C*), suggesting that the metabolic status of renal fibroblasts may switch to aerobic glycolytic program.

To identify the potential functional effect of enhanced aerobic glycolysis on the activation of renal myofibroblasts by TGF-β1, we blocked aerobic glycolysis in NRK-49F cells using glycolytic pathway inhibitor 2-DG or dichloroacetic acid (DCA) and then tested the activation of myofibroblasts by TGF-β1. In this experiment, NRK-49F cells were incubated with TGF-β1 in the presence or absence of 2-DG for 48 h. As expected, 2-DG treatment largely abolished the TGF-β1-induced increase of aerobic glycolysis in NRK-49F cells, which is reflected by decrease of pH of NRK-49F cell culture medium (Fig. 6*D*) but increase of both extracellular lactate level (Fig. 6*E*) and glucose consumption (Fig. 6*F*). Interestingly, Western blot analysis showed that 2-DG treatment dose-dependently abrogated the induction of FN, PCNA, and α-SMA expression

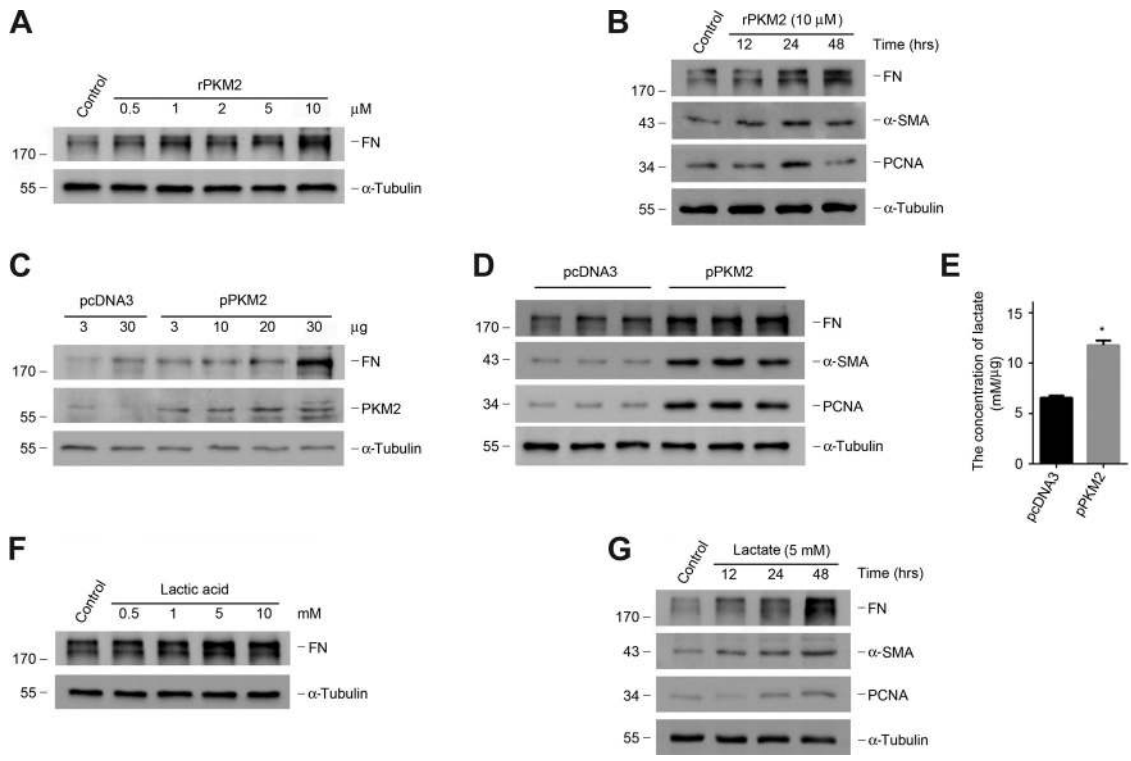

Fig. 5. Increased aerobic glycolysis is sufficient to cause myofibroblast activation. *A*: Western blot assay of FN and α-tubulin expression in NRK-49F cells incubated with rPKM2 for 48 h at different dosages. *B*: Western blot analysis showing FN, α-SMA, PCNA, and α-tubulin expression in NRK-49F cells incubated with 10 μM rPKM2 for different times. *C*: Western blot analysis showing FN and PKM2 expression in NRK-49F cells transfected with PKM2 plasmid for 72 h at different dosages. *D*: Western blot analysis showing FN, α-SMA, PCNA, and α-tubulin expression in NRK-49F cells transfected with 20-μg PKM2 plasmid for 72 h. *E*: lactate content normalized to protein in culture medium for cells in *D*. $^*P < 0.05$ compared with pcDNA3 group ($n = 6$). *F*: Western blot assay of FN and α-tubulin expression in NRK-49F cells incubated with lactate for 48 h at different dosages. *G*: Western blot analysis showing FN, α-SMA, PCNA, and α-tubulin expression in NRK-49F cells incubated with 5 mM lactate for different times.

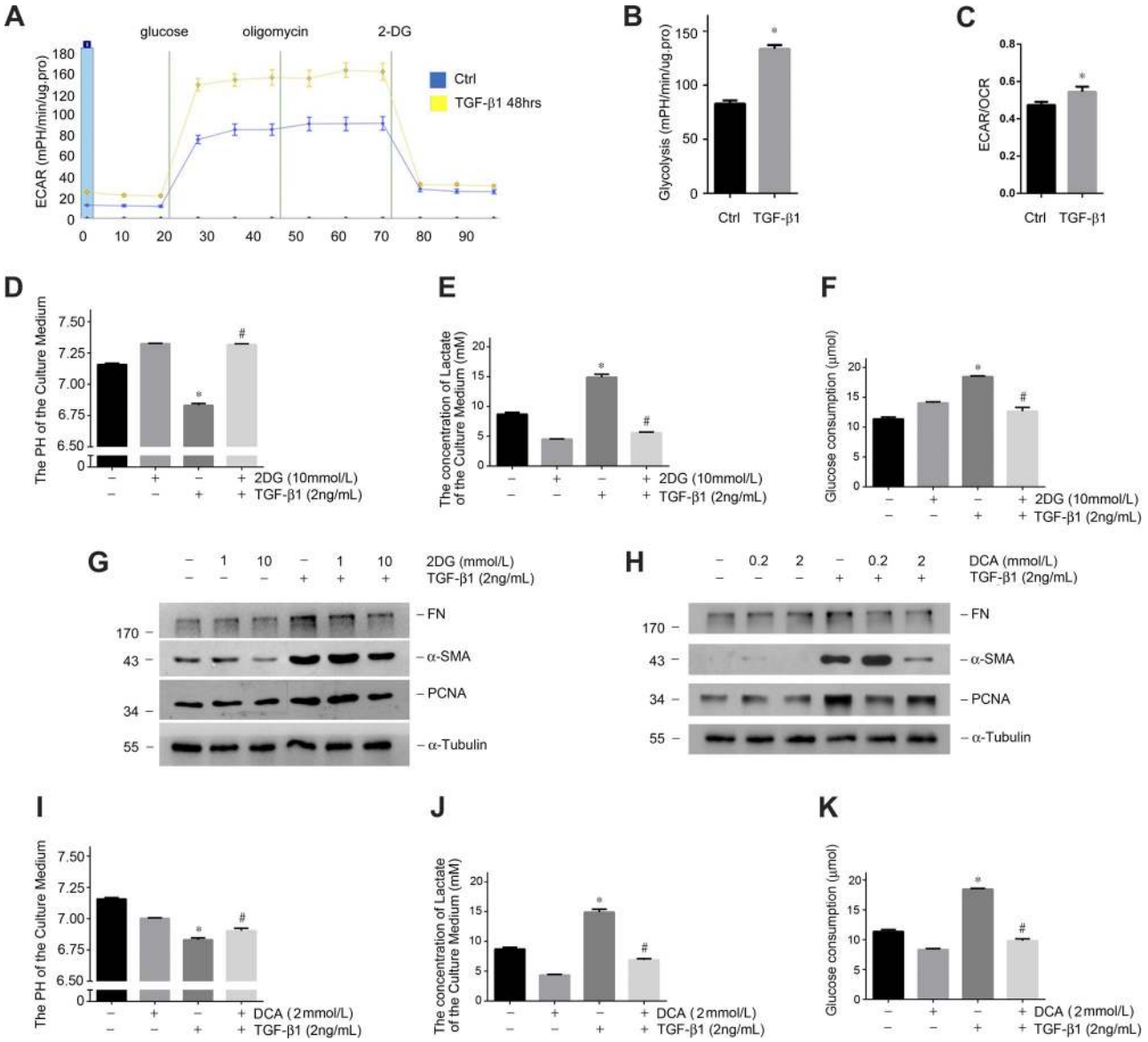

Fig. 6. Inhibition of aerobic glycolysis diminishes TGF-β1-induced myofibroblast activation. *A*: real-time ECAR of NRK-49F treated with 2 ng/ml TGF-β1 for 24 h, followed by sequential treatments with glucose, oligomycin, and 2-DG. Here, pro, protein. *B*: glycolytic capacity of NRK-49F cells incubated with TGF-β1 for 24 h. *C*: mean ratios of ECAR to OCR. *D–F*: NRK-49F cells were treated with TGF-β1 for 48 h in the absence or presence of 2-DG (10 mM). The pH (*D*) and lactate content (*E*) in culture medium and glucose consumption in NRK-49F cells (*F*) were determined. *G*: Western blot assay of FN, α-SMA, and PCNA in NRK-49F cells incubated with TGF-β1 (48 h) in the absence or presence of 2-DG (1 or 10 mM). *H*: Western blot assay of FN, α-SMA, and PCNA in NRK-49F cells incubated with TGF-β1 (48 h) in the absence or presence of DCA (0.2 or 2 mM). *I–K*: NRK-49F cells were treated with TGF-β1 (48 h) in the absence or presence of DCA (2 mM). The pH (*I*) and lactate content (*J*) in culture medium and glucose consumption in NRK-49F cells (*K*) were determined. $*P < 0.05$ compared with controls ($n = 5$ for *A–C* and $n = 8–10$ for *D–F* and *I–K*). $\#P < 0.05$ compared with NRK-49F cells treated with TGF-β1 in the absence of 2DG or DCA ($n = 8–10$ for *D–F* and *I–K*).

in NRK-49F cells by TGF-β1 (Fig. 6*G*). Consistent with this, DCA, another inhibitor of glycolysis, also abolished TGF-β1-induced myofibroblast activation. As shown in Fig. 6, *I–K*, DCA treatment remarkably increased the pH of culture medium of TGF-β1-treated NRK-49F cells (Fig. 6*I*) but decreased extracellular lactate content (Fig. 6*J*) and glucose consumption (Fig. 6*K*) of TGF-β1-treated NRK-49F cells. In a similar fashion, Western blot analysis showed that DCA treatment dose-dependently abolished the induction of FN, PCNA, and α-SMA expression in NRK-49F cells by TGF-β1 (Fig. 6*H*). These results collectively suggest that activation of renal myofibroblasts by TGF-β1 is tightly associated with an enhanced cellular aerobic glycolysis, and inhibition of aerobic glycolysis flow with glycolytic pathway inhibitor may suppress TGF-β1-induced myofibroblast activation.

Given that glycolysis inhibitors strongly suppress TGF-β1-induced renal myofibroblast activation in vitro, we ask whether glycolytic inhibition can attenuate renal fibrosis in mice with UUO surgery. In this experiment, we treated the UUO mice with 2-DG and compared the results with UUO mice and sham mice treated with vehicle only. Both Western blot assay and immunofluorescence staining showed that the UUO-induced FN abundance in mouse kidneys with 2-DG treatment was significantly less than in those without 2-DG treatment (Fig. 8,

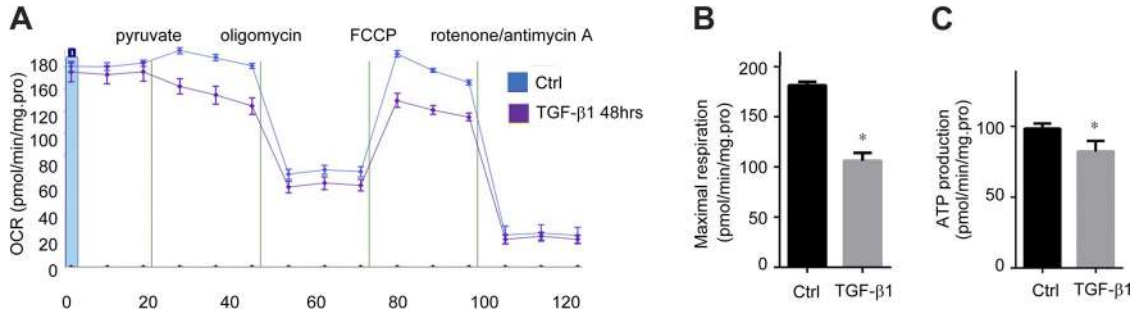

Fig. 7. *A*: real-time OCR of NRK-49F cells treated with 2 ng/ml TGF-β1 for 24 h, followed by sequential treatments with pyruvate, oligomycin, and FCCP. *B*: maximal respiration of NRK-49F cells incubated for 24 h with TGF-β1. *C*: ATP production of NRK-49F cells incubated with TGF-β1 for 24 h. $*P < 0.05$ compared with controls ($n = 5$).

A and *B*). Consistent with this, the renal morphology studies with hematoxylin and eosin and Sirius red demonstrated that 2-DG treatment significantly decreased the kidney tissue disruption and extracellular matrix accumulation induced by UUO surgery (Fig. 8*C*). Moreover, immunohistochemical analysis showed that the number of UUO-induced α-SMA and PCNA-positive myofibroblasts within the renal interstitium in the mouse group treated with 2-DG was remarkably decreased compared with that from the mouse group without 2-DG treatment (Fig. 8*C*). These results suggest that inhibitors of the glycolytic pathway can provide protection from UUO-induced renal fibrosis in a mouse model.

Shikonin attenuates renal fibrosis via inhibiting PKM2 expression and aerobic glycolysis. To confirm that blockade of aerobic glycolysis can suppress the development of UUO-induced renal fibrosis, we further tested whether downregulation of PKM2, the final rate-limiting glycolytic enzyme, can inhibit UUO-induced mouse renal fibrosis and TGF-β1-induced fibroblast activation. In this experiment, unilateral kidneys were injected with lentiviral PKM2 RNAi or lentiviral control RNAi 3 days before UUO surgery. The retroperitoneum was opened, and the left kidney was exposed. Then, 5×10^7 TU PKM RNAi lentiviral vectors were injected into the lower pole of the left kidney at several sites (55). As shown in Fig. 9, *A* and *B*, PKM2 expression was remarkably downregulated in fibrotic kidneys transfected with PKM2 RNAi compared with fibrotic kidneys transfected with vehicle. Downregulation of PKM2 in the kidney of mice with UUO surgery led to a significant reduction of FN, COL1A1, α-SMA, and PCNA expression in mouse kidneys (Fig. 9, *C* and *E*). Consistent with this, the total collagen content in the fibrotic kidneys following UUO surgery was also significantly decreased after knocking down PKM2 expression via PKM RNAi (Fig. 9*D*). Moreover, histology analysis confirmed that the mouse group treated with PKM RNAi displayed significantly less tubular damage as well as extracellular matrix deposition and PCNA-positive myofibroblasts within the renal interstitium compared with the mouse group treated with vehicle (Fig. 9*F*). NRK-49F cells were pretreated with different titers of lentiviral PKM RNAi for 12 h, followed by 48-h TGF-β1 (2 ng/ml) treatment. Western blot analysis showed that the expression of PKM2, FN, α-SMA, and PCNA in NRK-49F cells was decreased compared with control and vehicle group (Fig. 9, *G* and *H*).

Shikonin has recently been shown as an inhibitor for aerobic glycolysis and PKM2 expression (3) in blocking macrophage secretion and tumor proliferation. Given that PKM2-mediated metabolic switch to aerobic glycolysis plays an essential role in promoting renal fibrosis, we tested whether the administration of shikonin could attenuate renal fibrosis in mice with UUO surgery. In this experiment, Shikonin was intragastrically administered at various doses (1 or 5 mg/kg body wt) 1 day before UUO surgery and also administered daily for 7 consecutive days. As shown in Fig. 10, *A* and *B*, shikonin dose-dependently reduced the expression of both PKM2 and p-PKM2 in fibrotic kidneys of mice with UUO surgery. As a consequence, the UUO-induced expression of FN, COL1A1, α-SMA, and PCNA (Fig. 10, *C* and *D*) and amount of collagen deposition (Fig. 10*E*) in the kidney tissues were decreased by shikonin in a dose-dependent manner. Histological analysis of mouse kidneys also showed that administration of shikonin effectively mitigated the tissue disruption induced by UUO surgery (Fig. 10*F*).

DISCUSSION

In the present study, we show that glycolytic suppression can diminish TGF-β1-induced myofibroblast activation and attenuates UUO-induced renal fibrosis. Our findings not only identify a crucial role of enhanced aerobic glycolysis in renal myofibroblast activation and development of renal fibrosis in mice with UUO surgery but also provide specific glycolytic inhibitors such as shikonin and 2-DG as a potential novel strategy for treating renal fibrosis.

Although all cell types in the kidneys are involved in the pathogenesis of kidney fibrosis, fibroblasts, which acquire the phenotype of myofibroblast and generate a large amount of interstitial matrix upon activation, are the principal matrix-producing cells (1a, 7, 26). Therefore we used renal fibroblast as a cell model to study the effect of aerobic glycolysis on renal fibrosis. We performed both in vitro and in vivo studies using TGF-β1-treated renal fibroblasts and mice with UUO surgery, respectively. During fibrosis, renal fibroblasts generally initiated two main processes: proliferation and extracellular matrix synthesis. Both proliferation and extracellular matrix synthesis would force fibroblasts to produce not only necessary ATP but more importantly, the materials such as amino acid and nucleotide for making new molecules or cells. Since aerobic glycolysis can provide both necessary ATP and sufficient metabolic intermediates as materials for synthesis (43), fibroblasts switching the metabolic profile from oxidative phosphorylation to aerobic glycolysis may be a necessary prerequisite for

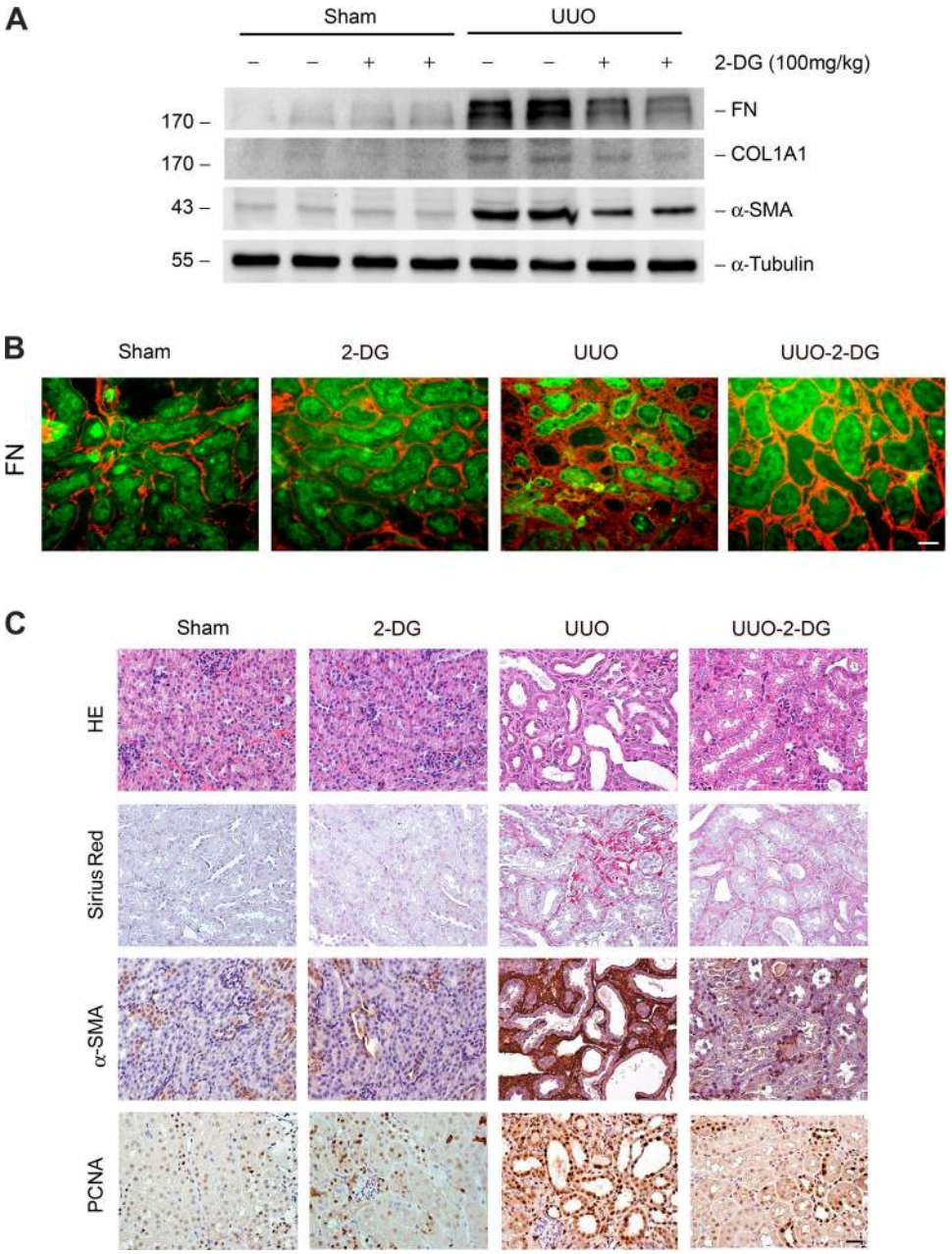

Fig. 8. Inhibition of glycolysis therapeutically attenuates UUO-induced renal fibrosis. *A*: Western blot assay of FN, COL1A1, and α-SMA expression. 2-DG (100 mg/kg body wt) was administered intraperitoneally daily for 8 days; sham-operated mice were used as controls. Kidneys were harvested at 7 days post-UUO surgery. *B*: immunofluorescence staining showing the colocalization of laminin and FN in fibrotic kidney. Scale bar = 20 μm. *C*: representative hematoxylin and eosin, Sirius red, α-SMA, and PCNA staining of kidney morphology, collagen deposition, and myofibroblast activation in each group. Scale bar = 20 μm.

fibroblasts to synthesize extracellular matrix and to further proliferate.

Aerobic glycolysis (also termed "Warburg effect") has been well established as a major feature of tumor cell metabolism (6, 20, 43). In fast-proliferating cancer cells, aerobic glycolysis converts each glucose molecule to two ATP and various metabolic intermediate products, which is necessary for the synthesis of new proteins and genetic materials. Blockade of aerobic glycolysis flow, particularly PKM2-mediated metabolic switch, in tumor cells has shown a great potential in antitumor therapy (51). Metabolic perturbation has also been implicated in the pathogenesis of a number of kidney diseases (5, 37). Rowe et al. (37) reported a shift of metabolism profile toward aerobic glycolysis during PKD pathogenesis. Employing orthologous and slowly progressive murine models, Chiaravalli et al. (5) demonstrated that 2-DG greatly delayed PKD progression in both model systems. On the basis of these studies, we hypothesized that altered glucose metabolism may also be a feature of renal myofibroblast activation during kidney fibrosis. To test this, we performed analysis using the Seahorse X24 Extracellular Flux Analyzer and observed that ECAR was markedly increased and OCR was significantly decreased after 48-h treatment with TGF-β1, confirming that the metabolic status of renal fibroblasts was switched to the aerobic glycolytic program. Glucose metabolism disturbance was further confirmed in TGF-β1-treated NRK-49F fibroblasts. Furthermore, we found that the level of PKM2, particularly p-PKM2, in the fibrotic kidneys was significantly upregulated compared with that in sham controls.

Current therapeutic options for CKD and renal fibrosis in the clinical setting are scarce (26). Given an essential role of metabolic perturbation in renal fibrosis, particularly the signif-

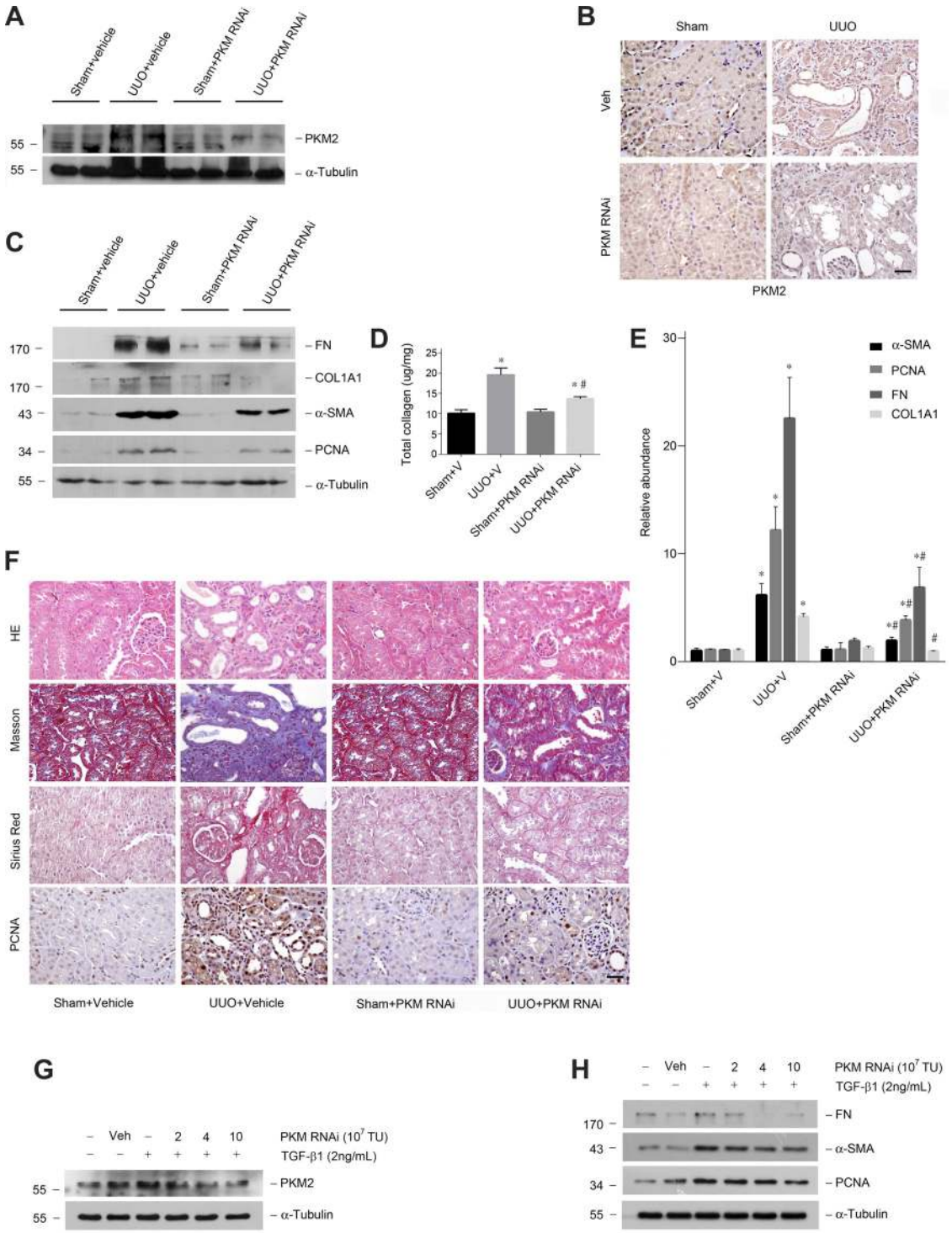

Fig. 9. PKM2 knockdown via lentiviral PKM2 RNAi attenuates renal fibrosis. *A*: Western blot assay of PKM2 in each group. Mice were administered with lentiviral PKM2 RNAi or vehicle 3 days before UUO surgery. Kidneys were harvested on *day 7* post-UUO. Sham-operated mice were used as controls. *B*: representative immunohistochemical staining of PKM2 in kidneys. Signals were visualized by horseradish peroxidase and 3,3'-diaminobenzidine. Scale bar = 20 μm. *C*: Western blot analysis of FN, COL1A1, α-SMA, and PCNA in kidneys. *D* and *E*: graphic presentation of total collagen (*D*), as well as α-SMA, PCNA, FN, and COL1A1 levels normalized to α-tubulin (*E*) in kidneys from different groups. $*P < 0.05$ compared with sham controls ($n = 4$); $\#P < 0.05$ compared with UUO nephropathy group ($n = 4$). *F*: representative hematoxylin and eosin, Masson trichrome, Sirius red, and PCNA staining showing kidney morphology, interstitial fibrosis, collagen deposition, and myofibroblast activation. Scale bar = 20 μm. *G*: Western blot analysis of PKM2 in NRK-49F cells pretreated with different titers of lentiviral PKM2 RNAi for 12 h, followed by TGF-β1 (2 ng/ml) treatment for 48 h. *H*: Western blot analysis of FN, α-SMA, and PCNA. V and Veh, vehicle.

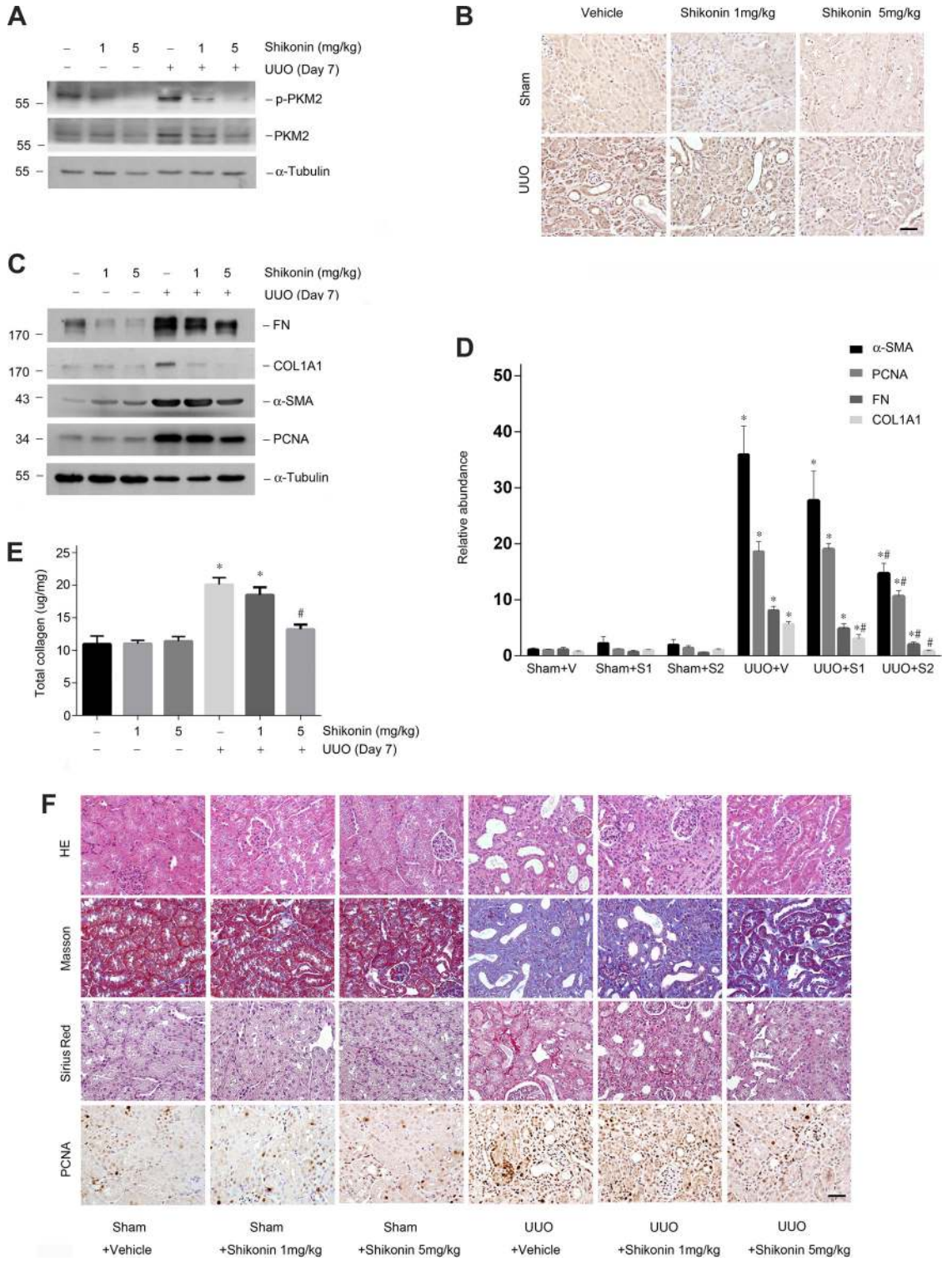

Fig. 10. Shikonin inhibits PKM2 expression and attenuates renal fibrosis. *A*: Western blot analysis of renal p-PKM2 and PKM2 levels in each group. Shikonin (1 or 5 mg/kg body wt) was intragastrically administered daily for 8 days. Kidneys were harvested on *day 7* post-UUO surgery. *B*: representative immunohistochemical staining of PKM2 in the kidneys. Scale bar = 20 μm. *C*: Western blot analysis of FN, COL1A1, α-SMA, and PCNA in the kidneys of each group. *D*: graphic presentation of α-SMA, PCNA, FN, and COL1A1 levels normalized to α-tubulin. S1 and S2, 1 and 5 mg/kg body wt shikonin dosage, respectively. $*P < 0.05$ compared with sham controls ($n = 4$); $\#P < 0.05$ compared with UUO nephropathy group ($n = 4$). *E*: graphic presentation of total collagen content in the kidneys in different groups. $*P < 0.05$ compared with sham controls ($n = 4$); $\#P < 0.05$ compared with UUO nephropathy group ($n = 4$). *F*: representative hematoxylin and eosin, Masson trichrome, Sirius red, and PCNA staining for kidney morphology interstitial fibrosis, collagen deposition, and myofibroblast activation. Scale bar = 20 μm.

icantly increased level of phosphorylated PKM2 in both fibrotic kidneys and activated myofibroblasts, we speculated that reduction of PKM2 phosphorylation or blockade of glycolytic flux might present a new strategy to delay the renal fibrosis process. Our data showed that knockdown of PKM2 expression by transfection with lentiviral PKM2 siRNA or administration with shikonin significantly mitigated the kidney tissue disruption induced by UUO surgery. Moreover, decrease of PKM2 expression by shikonin treatment also markedly reduced the production of FN, COL1A1, α-SMA, and PCNA and deposition of collagen in kidney tissues from mice with UUO surgery. More importantly, immunostaining analysis of human renal tissue samples further showed that PKM2 expression in kidney interstitium was also positively correlated with the progression of renal fibrosis in patients with different degrees of renal fibrosis, suggesting that PKM2 may be involved in the progression of renal fibrosis in CKD patients.

In addition to the role in switching cellular metabolic profile to aerobic glycolysis, PKM2 has been shown to serve as a transcriptional coactivator (27, 52) and involved in many other cell functions (18). Furthermore, both expression and enzymatic activity of PKM2 are regulated at different levels, including transcription, pre-mRNA slicing, miRNA-regulated mRNA stability, protein stability, posttranslational modifications, and allosteric regulation (51). Therefore the specific mechanisms of how PKM2 is dysregulated during myofibroblast activation or kidney fibrosis and how upregulated PKM2 affects myofibroblast activation and renal fibrosis are of great interest and require further investigation.

We also showed that other glycolysis inhibitors such as 2-DG and DCA effectively diminished TGF-β1-induced myofibroblast activation and ameliorated kidney tissue disruption and fibrosis progression in mice with UUO surgery. These results are in agreement with previous reports that 2-DG ameliorated the histology and cystic index of kidneys from PKD mouse models (5, 37). Moreover, not only using a preventive protocol in which inhibitors were given before surgery, we determined that 2-DG and shikonin are still effective when kidney injury is already established (data not shown). 2-DG is a glucose molecule that has the 2-hydroxyl group replaced by hydrogen, so that it cannot undergo further glycolysis. Clinical trials confirmed that the administration of 2-DG alone or combined with other anticancer therapies, such as chemotherapy and radiotherapy, was safe and well tolerated by patients. As a monotherapy, 2-DG was investigated in clinical trials in the late 1950s based on Warburg's observation, though the results were discouraging (21). Recently, a phase I clinical trial showed that 2-DG at 63 mg/kg in combination with weekly docetaxel was well tolerated in patients with advanced solid tumors (36). 2-DG is commonly thought to inhibit glycolysis; however, it actually has related and integrated metabolic effects and impedes various biological processes, such as depletion of cellular energy, aggravation of oxidative stress, interference with N-linked glycosylation, and induction of autophagy (1, 15), which also activates multiple signaling pathways, including the phosphatidylinositol 3-kinases, MAPK, and AMPK (19, 49). Although 2-DG is not currently approved for any human condition, its low toxicity but high efficiency in ameliorating renal fibrosis make 2-DG another candidate for further testing in humans suffering from CKD.

Shikonin is one of the active components of zicao, the root extract of *Lithospermum erythrorhizon*. Studies performed over the past three decades have demonstrated that shikonin and its derivatives are able to act simultaneously on various targets, which represents a great advantage in the treatment of different diseases (45). They are potent pharmaceutical substances with interesting pharmacological properties including wound-healing, anticancer (50), antibacterial (33), anti-inflammatory (42), antiviral (4), and other biological activities. Recently, shikonin has been shown as a class of novel PKM2 inhibitors which effectively inhibited the cellular glycolytic flux dominantly expressing PKM2. Interestingly, shikonin showed a promising selectivity toward PKM2 (3). We showed that shikonin dose-dependently reduced the expression of both PKM2 and p-PKM2 in fibrotic kidneys of mice with UUO surgery and effectively mitigated the tissue disruption.

In summary, our study demonstrated that a switch of metabolism from oxidative phosphorylation to aerobic glycolysis in renal fibroblasts was the primary feature of fibroblast activation during renal fibrosis and that suppressing renal fibroblast aerobic glycolysis, particularly the cellular level of PKM2 phosphorylation, could significantly reduce renal fibrosis. Our findings thus provide novel potential therapeutic strategies for treating renal fibrosis.

GRANTS

This work was supported by 973 Science Program of the Ministry of Science and Technology of China (2012CB517603), National Science Foundation of China Grant 81470971, Key Project of National Natural Science Foundation of China 81530022, National Science Foundation of China Grant 31300955/C1102 (J. Lei), and Science Foundation of Jiangsu Province Grant BK-20141489 (J. Lei).

DISCLOSURES

No conflicts of interest, financial or otherwise, are declared by the authors.

AUTHOR CONTRIBUTIONS

H.D., L.J., and J.Y. conceived and designed research; H.D., L.J., J.X., F.B., Y.Z., and K.Z. performed experiments; H.D., L.J., Q.Y., and J.L. analyzed data; H.D. interpreted results of experiments; H.D. and L.J. prepared figures; H.D. and K.Z. drafted manuscript; H.D., L.J., and J.Y. edited and revised manuscript; J.Y. approved final version of manuscript.

REFERENCES

1. **Bandugula VR, N RP.** 2-Deoxy-D-glucose and ferulic acid modulates radiation response signaling in non-small cell lung cancer cells. *Tumour Biol* 34: 251–259, 2013. doi:10.1007/s13277-012-0545-6.
1a. **Boor P, Ostendorf T, Floege J.** Renal fibrosis: novel insights into mechanisms and therapeutic targets. *Nat Rev Nephrol* 6: 643–656, 2010. doi:10.1038/nrneph.2010.120.
2. **Bradshaw AD.** The role of SPARC in extracellular matrix assembly. *J Cell Commun Signal* 3: 239–246, 2009. doi:10.1007/s12079-009-0062-6.
3. **Chen J, Xie J, Jiang Z, Wang B, Wang Y, Hu X.** Shikonin and its analogs inhibit cancer cell glycolysis by targeting tumor pyruvate kinase-M2. *Oncogene* 30: 4297–4306, 2011. doi:10.1038/onc.2011.137.
4. **Chen X, Yang L, Oppenheim JJ, Howard MZ.** Cellular pharmacology studies of shikonin derivatives. *Phytother Res* 16: 199–209, 2002. doi:10.1002/ptr.1100.
5. **Chiaravalli M, Rowe I, Mannella V, Quilici G, Canu T, Bianchi V, Gurgone A, Antunes S, D'Adamo P, Esposito A, Musco G, Boletta A.** 2-Deoxy-D-glucose ameliorates PKD progression. *J Am Soc Nephrol* 27: 1958–1969, 2016. doi:10.1681/ASN.2015030231.
6. **DeBerardinis RJ, Lum JJ, Hatzivassiliou G, Thompson CB.** The biology of cancer: metabolic reprogramming fuels cell growth and proliferation. *Cell Metab* 7: 11–20, 2008. doi:10.1016/j.cmet.2007.10.002.

7. **Duffield JS.** Cellular and molecular mechanisms in kidney fibrosis. *J Clin Invest* 124: 2299–2306, 2014. doi:10.1172/JCI72267.
8. **Duffield JS.** Macrophages in kidney repair and regeneration. *J Am Soc Nephrol* 22: 199–201, 2011. doi:10.1681/ASN.2010121301.
9. **Duranton F, Lundin U, Gayrard N, Mischak H, Aparicio M, Mourad G, Daurès JP, Weinberger KM, Argilés A.** Plasma and urinary amino acid metabolomic profiling in patients with different levels of kidney function. *Clin J Am Soc Nephrol* 9: 37–45, 2014. doi:10.2215/CJN.06000613.
10. **Eddy AA.** Progression in chronic kidney disease. *Adv Chronic Kidney Dis* 12: 353–365, 2005. doi:10.1053/j.ackd.2005.07.011.
11. **Ferrick DA, Neilson A, Beeson C.** Advances in measuring cellular bioenergetics using extracellular flux. *Drug Discov Today* 13: 268–274, 2008. doi:10.1016/j.drudis.2007.12.008.
12. **Floege J, Eitner F, Alpers CE.** A new look at platelet-derived growth factor in renal disease. *J Am Soc Nephrol* 19: 12–23, 2008. doi:10.1681/ASN.2007050532.
13. **Gandolfo MT, Jang HR, Bagnasco SM, Ko GJ, Agreda P, Satpute SR, Crow MT, King LS, Rabb H.** Foxp3+ regulatory T cells participate in repair of ischemic acute kidney injury. *Kidney Int* 76: 717–729, 2009. doi:10.1038/ki.2009.259.
14. **Gao X, Wang H, Yang JJ, Chen J, Jie J, Li L, Zhang Y, Liu ZR.** Reciprocal regulation of protein kinase and pyruvate kinase activities of pyruvate kinase M2 by growth signals. *J Biol Chem* 288: 15971–15979, 2013. doi:10.1074/jbc.M112.448753.
15. **Giammarioli AM, Gambardella L, Barbati C, Pietraforte D, Tinari A, Alberton M, Gnessi L, Griffin RJ, Minetti M, Malorni W.** Differential effects of the glycolysis inhibitor 2-deoxy-D-glucose on the activity of pro-apoptotic agents in metastatic melanoma cells, and induction of a cytoprotective autophagic response. *Int J Cancer* 131: E337–E347, 2012. doi:10.1002/ijc.26420.

15a. **Grande MT, López-Novoa JM.** Fibroblast activation and myofibroblast generation in obstructive nephropathy. *Nat Rev Nephrol* 5: 319–328, 2009. doi:10.1038/nrneph.2009.74.

16. **Inoue T, Takenaka T, Hayashi M, Monkawa T, Yoshino J, Shimoda K, Neilson EG, Suzuki H, Okada H.** Fibroblast expression of an IκB dominant-negative transgene attenuates renal fibrosis. *J Am Soc Nephrol* 21: 2047–2052, 2010. doi:10.1681/ASN.2010010003.
17. **Jha V, Garcia-Garcia G, Iseki K, Li Z, Naicker S, Plattner B, Saran R, Wang AY-M, Yang C-W.** Chronic kidney disease: global dimension and perspectives. *Lancet* 382: 260–272, 2013. doi:10.1016/S0140-6736(13)60687-X.
18. **Jiang Y, Wang Y, Wang T, Hawke DH, Zheng Y, Li X, Zhou Q, Majumder S, Bi E, Liu DX, Huang S, Lu Z.** PKM2 phosphorylates MLC2 and regulates cytokinesis of tumour cells. *Nat Commun* 5: 5566, 2014. doi:10.1038/ncomms6566.
19. **Kim SM, Yun MR, Hong YK, Solca F, Kim JH, Kim HJ, Cho BC.** Glycolysis inhibition sensitizes non-small cell lung cancer with T790M mutation to irreversible EGFR inhibitors via translational suppression of Mcl-1 by AMPK activation. *Mol Cancer Ther* 12: 2145–2156, 2013. doi:10.1158/1535-7163.MCT-12-1188.
20. **Koppenol WH, Bounds PL, Dang CV.** Otto Warburg's contributions to current concepts of cancer metabolism. *Nat Rev Cancer* 11: 325–337, 2011. doi:10.1038/nrc3038.
21. **Landau BR, Laszlo J, Stengle J, Burk D.** Certain metabolic and pharmacologic effects in cancer patients given infusions of 2-deoxy-D-glucose. *J Natl Cancer Inst* 21: 485–494, 1958.
22. **Li J, Ren J, Liu X, Jiang L, He W, Yuan W, Yang J, Dai C.** Rictor/mTORC2 signaling mediates TGFβ1-induced fibroblast activation and kidney fibrosis. *Kidney Int* 88: 515–527, 2015. doi:10.1038/ki.2015.119.
23. **Li L, Zhang Y, Qiao J, Yang JJ, Liu ZR.** Pyruvate kinase M2 in blood circulation facilitates tumor growth by promoting angiogenesis. *J Biol Chem* 289: 25812–25821, 2014. doi:10.1074/jbc.M114.576934.
24. **Lin SL, Kisseleva T, Brenner DA, Duffield JS.** Pericytes and perivascular fibroblasts are the primary source of collagen-producing cells in obstructive fibrosis of the kidney. *Am J Pathol* 173: 1617–1627, 2008. doi:10.2353/ajpath.2008.080433.
25. **Liu N, Guo JK, Pang M, Tolbert E, Ponnusamy M, Gong R, Bayliss G, Dworkin LD, Yan H, Zhuang S.** Genetic or pharmacologic blockade of EGFR inhibits renal fibrosis. *J Am Soc Nephrol* 23: 854–867, 2012. doi:10.1681/ASN.2011050493.
26. **Liu Y.** Cellular and molecular mechanisms of renal fibrosis. *Nat Rev Nephrol* 7: 684–696, 2011. doi:10.1038/nrneph.2011.149.
27. **Lv L, Xu YP, Zhao D, Li FL, Wang W, Sasaki N, Jiang Y, Zhou X, Li TT, Guan KL, Lei QY, Xiong Y.** Mitogenic and oncogenic stimulation of K433 acetylation promotes PKM2 protein kinase activity and nuclear localization. *Mol Cell* 52: 340–352, 2013. doi:10.1016/j.molcel.2013.09.004.
30. **Niewczas MA, Sirich TL, Mathew AV, Skupien J, Mohney RP, Warram JH, Smiles A, Huang X, Walker W, Byun J, Karoly ED, Kensicki EM, Berry GT, Bonventre JV, Pennathur S, Meyer TW, Krolewski AS.** Uremic solutes and risk of end-stage renal disease in type 2 diabetes: metabolomic study. *Kidney Int* 85: 1214–1224, 2014. doi:10.1038/ki.2013.497.
31. **Nightingale J, Patel S, Suzuki N, Buxton R, Takagi KI, Suzuki J, Sumi Y, Imaizumi A, Mason RM, Zhang Z.** Oncostatin M, a cytokine released by activated mononuclear cells, induces epithelial cell-myofibroblast transdifferentiation via Jak/Stat pathway activation. *J Am Soc Nephrol* 15: 21–32, 2004. doi:10.1097/01.ASN.0000102479.92582.43.
32. **Paliege A, Rosenberger C, Bondke A, Sciesielski L, Shina A, Heyman SN, Flippin LA, Arend M, Klaus SJ, Bachmann S.** Hypoxia-inducible factor-2alpha-expressing interstitial fibroblasts are the only renal cells that express erythropoietin under hypoxia-inducible factor stabilization. *Kidney Int* 77: 312–318, 2010. doi:10.1038/ki.2009.460.
33. **Papageorgiou VP.** Naturally occurring isohexenylnaphthazarin pigments: a new class of drugs. *Planta Med* 38: 193–203, 1980. doi:10.1055/s-2008-1074864.
34. **Pena MJ, Lambers Heerspink HJ, Hellemons ME, Friedrich T, Dallmann G, Lajer M, Bakker SJL, Gansevoort RT, Rossing P, de Zeeuw D, Roscioni SS.** Urine and plasma metabolites predict the development of diabetic nephropathy in individuals with type 2 diabetes mellitus. *Diabet Med* 31: 1138–1147, 2014. doi:10.1111/dme.12447.
35. **Posada-Ayala M, Zubiri I, Martin-Lorenzo M, Sanz-Maroto A, Molero D, Gonzalez-Calero L, Fernandez-Fernandez B, de la Cuesta F, Laborde CM, Barderas MG, Ortiz A, Vivanco F, Alvarez-Llamas G.** Identification of a urine metabolomic signature in patients with advanced-stage chronic kidney disease. *Kidney Int* 85: 103–111, 2014. doi:10.1038/ki.2013.328.
36. **Raez LE, Papadopoulos K, Ricart AD, Chiorean EG, Dipaola RS, Stein MN, Rocha Lima CM, Schlesselman JJ, Tolba K, Langmuir VK, Kroll S, Jung DT, Kurtoglu M, Rosenblatt J, Lampidis TJ.** A phase I dose-escalation trial of 2-deoxy-D-glucose alone or combined with docetaxel in patients with advanced solid tumors. *Cancer Chemother Pharmacol* 71: 523–530, 2013. doi:10.1007/s00280-012-2045-1.
37. **Rowe I, Chiaravalli M, Mannella V, Ulisse V, Quilici G, Pema M, Song XW, Xu H, Mari S, Qian F, Pei Y, Musco G, Boletta A.** Defective glucose metabolism in polycystic kidney disease identifies a new therapeutic strategy. *Nat Med* 19: 488–493, 2013. doi:10.1038/nm.3092.
38. **Shah VO, Townsend RR, Feldman HI, Pappan KL, Kensicki E, Vander Jagt DL.** Plasma metabolomic profiles in different stages of CKD. *Clin J Am Soc Nephrol* 8: 363–370, 2013. doi:10.2215/CJN.05540512.
39. **Shweke N, Boulos N, Jouanneau C, Vandermeersch S, Melino G, Dussaule JC, Chatziantoniou C, Ronco P, Boffa JJ.** Tissue transglutaminase contributes to interstitial renal fibrosis by favoring accumulation of fibrillar collagen through TGF-beta activation and cell infiltration. *Am J Pathol* 173: 631–642, 2008. doi:10.2353/ajpath.2008.080025.
40. **Souma T, Yamazaki S, Moriguchi T, Suzuki N, Hirano I, Pan X, Minegishi N, Abe M, Kiyomoto H, Ito S, Yamamoto M.** Plasticity of renal erythropoietin-producing cells governs fibrosis. *J Am Soc Nephrol* 24: 1599–1616, 2013. doi:10.1681/ASN.2013010030.
41. **Strutz F, Zeisberg M.** Renal fibroblasts and myofibroblasts in chronic kidney disease. *J Am Soc Nephrol* 17: 2992–2998, 2006. doi:10.1681/ASN.2006050420.
42. **Tanaka S, Tajima M, Tsukada M, Tabata M.** A comparative study on anti-inflammatory activities of the enantiomers, shikonin and alkannin. *J Nat Prod* 49: 466–469, 1986. doi:10.1021/np50045a014.
43. **Vander Heiden MG, Cantley LC, Thompson CB.** Understanding the Warburg effect: the metabolic requirements of cell proliferation. *Science* 324: 1029–1033, 2009. doi:10.1126/science.1160809.
44. **Wang P, Sun C, Zhu T, Xu Y.** Structural insight into mechanisms for dynamic regulation of PKM2. *Protein Cell* 6: 275–287, 2015. doi:10.1007/s13238-015-0132-x.
45. **Wang R, Yin R, Zhou W, Xu D, Li S.** Shikonin and its derivatives: a patent review. *Expert Opin Ther Pat* 22: 977–997, 2012. doi:10.1517/13543776.2012.709237.

46. **Wang Z, Ying Z, Bosy-Westphal A, Zhang J, Schautz B, Later W, Heymsfield SB, Müller MJ.** Specific metabolic rates of major organs and tissues across adulthood: evaluation by mechanistic model of resting energy expenditure. *Am J Clin Nutr* 92: 1369–1377, 2010. doi:10.3945/ajcn.2010.29885.
47. **Wynn TA.** Common and unique mechanisms regulate fibrosis in various fibroproliferative diseases. *J Clin Invest* 117: 524–529, 2007. doi:10.1172/JCI31487.
48. **Yamaguchi I, Tchao BN, Burger ML, Yamada M, Hyodo T, Giampietro C, Eddy AA.** Vascular endothelial cadherin modulates renal interstitial fibrosis. *Nephron, Exp Nephrol* 120: e20–e31, 2012. doi:10.1159/000332026.
49. **Yamaguchi R, Janssen E, Perkins G, Ellisman M, Kitada S, Reed JC.** Efficient elimination of cancer cells by deoxyglucose-ABT-263/737 combination therapy. *PLoS One* 6: e24102, 2011. doi:10.1371/journal.pone.0024102.
50. **Yang H, Zhou P, Huang H, Chen D, Ma N, Cui QC, Shen S, Dong W, Zhang X, Lian W, Wang X, Dou QP, Liu J.** Shikonin exerts antitumor activity via proteasome inhibition and cell death induction in vitro and in vivo. *Int J Cancer* 124: 2450–2459, 2009. doi:10.1002/ijc.24195.
51. **Yang W, Lu Z.** Pyruvate kinase M2 at a glance. *J Cell Sci* 128: 1655–1660, 2015. doi:10.1242/jcs.166629.
52. **Yang W, Zheng Y, Xia Y, Ji H, Chen X, Guo F, Lyssiotis CA, Aldape K, Cantley LC, Lu Z.** ERK1/2-dependent phosphorylation and nuclear translocation of PKM2 promotes the Warburg effect. *Nat Cell Biol* 14: 1295–1304, 2012. doi:10.1038/ncb2629.
53. **Yu B, Zheng Y, Nettleton JA, Alexander D, Coresh J, Boerwinkle E.** Serum metabolomic profiling and incident CKD among African Americans. *Clin J Am Soc Nephrol* 9: 1410–1417, 2014. doi:10.2215/CJN.11971113.
54. **Zhang L, Wang F, Wang L, Wang W, Liu B, Liu J, Chen M, He Q, Liao Y, Yu X, Chen N, Zhang JE, Hu Z, Liu F, Hong D, Ma L, Liu H, Zhou X, Chen J, Pan L, Chen W, Wang W, Li X, Wang H.** Prevalence of chronic kidney disease in China: a cross-sectional survey. *Lancet* 379: 815–822, 2012. doi:10.1016/S0140-6736(12)60033-6.
55. **Zhou C, Shan Y, Zhao H, He P.** Biological effects of lentivirus-mediated shRNA targeting collagen type I on the mesangial cells of rats. *Ren Fail* 33: 334–340, 2011. doi:10.3109/0886022X.2011.559679.
56. **Zhou L, Li Y, Zhou D, Tan RJ, Liu Y.** Loss of Klotho contributes to kidney injury by derepression of Wnt/β-catenin signaling. *J Am Soc Nephrol* 24: 771–785, 2013. doi:10.1681/ASN.2012080865.